JACS
JOURNAL OF THE AMERICAN CHEMICAL SOCIETY
Article
Cite This: J. Am. Chem. Soc. 2018, 140, 13478−13487
pubs.acs.org/JACS

Hierarchical Self-Organization of Chiral Columns from Chiral Supramolecular Spheres

Dipankar Sahoo,[†,⊥] Mohammad R. Imam,[†,¶] Mihai Peterca,[†,‡] Benjamin E. Partridge,[†] Daniela A. Wilson,[†,#] Xiangbing Zeng,[§] Goran Ungar,[§,∥] Paul A. Heiney,[‡] and Virgil Percec*[,†]

[†]Roy & Diana Vagelos Laboratories, Department of Chemistry, University of Pennsylvania, Philadelphia, Pennsylvania 19104-6323, United States

[‡]Department of Physics and Astronomy, University of Pennsylvania, Philadelphia, Pennsylvania 19104-6396, United States

[§]Department of Materials Science and Engineering, University of Sheffield, Sheffield, S1 3JD, United Kingdom

[∥]Department of Physics, Zhejiang Sci-Tech University, 310018 Hangzhou, China

Supporting Information

ABSTRACT: The supramolecular column is an archetypal architecture in the field of periodic liquid crystalline and crystalline arrays. Columns are generated via self-assembly, coassembly, and polymerization of monomers containing molecules shaped as discs, tapered, twin- and Janus-tapered, crowns, hat-shaped crowns, and fragments thereof. These supramolecular columns can be helical and therefore exhibit chirality. In contrast, spheres represent a fundamentally distinct architecture, generated from conical and crown-like molecules, which self-organize into body-centered cubic, $Pm\bar{3}n$ cubic (also known as Frank−Kasper A15), and tetragonal (also known as Frank−Kasper σ) phases. Supramolecular spherical aggregates are not known to further assemble into a columnar architecture, except as an intermediate state between a columnar periodic array and a cubic phase. In the present work, a chiral dendronized cyclotetraveratrylene (CTTV) derivative is demonstrated to self-organize into a supramolecular column unexpectedly constructed from supramolecular spheres, with no subsequent transition to a cubic phase. Structural and retrostructural analysis using a combination of differential scanning calorimetry, X-ray diffraction (XRD), molecular modeling, and simulation of XRD patterns reveals that this CTTV derivative, which is functionalized with eight chiral first-generation minidendrons, self-organizes via a column-from-spheres model. The transition from column to column-from-spheres was monitored by circular dichroism spectroscopy, which demonstrated that both the supramolecular column and supramolecular spheres are chiral. This column-from-spheres model, which unites two fundamentally distinct self-assembled architectures, provides a new mechanism to self-organize supramolecular columnar architectures.

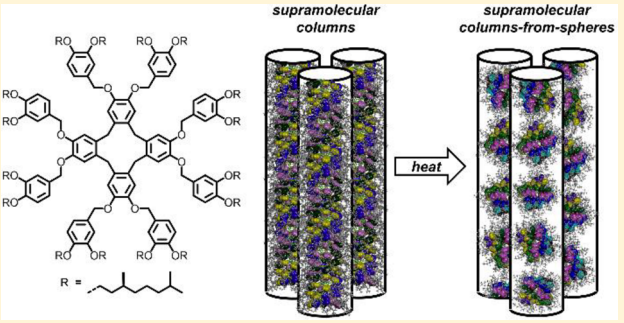

INTRODUCTION

The self-assembly of supramolecular columns from disc-like molecules is well established.[1] Subsequently, tapered,[2] twin-tapered,[3] and Janus-tapered[4] molecules and larger fragments of discs,[5] as well as other quasi-discotic molecules including crown-like molecules[6] and hat-shaped crowns,[6c] were also demonstrated to self-assemble into supramolecular columns by various combinations of nonbonding interactions[7] or by polymerization.[8] These columns self-organize into periodic liquid crystalline and crystalline arrays that exhibit diverse functions including ionic and electronic conduction,[9] nanomechanical function,[10] water transport as mimics of transmembrane pores,[11] and nanoporous polymer films.[12] In contrast, supramolecular spheres cannot be self-assembled from tapered molecules and flat discs, or fragments thereof, unless those molecules are able to undergo conformational changes. Such *quasiequivalent*[13] building blocks and dendronized components adopting a conical or crown-like conformation may self-assemble into supramolecular spheres,[1j,l] which subsequently self-organize into 3D phases including body-centered cubic (BCC, $Im\bar{3}m$),[14] $Pm\bar{3}n$ cubic[15] (known also as Frank−Kasper A15[16] or Q_{223}[17]), tetragonal ($P4_2/mnm$, known also as Frank−Kasper σ),[18] and 12-fold liquid quasicrystalline (LQC)[16b,19] phases. Notably, helical supramolecular columns and supramolecular spheres can be chiral,[8d,10c,20,21] even when they are assembled from achiral dendrons.[1j,l] The chirality of a sphere, which can most easily be conceived as a loxodrome that resembles a helical apple peel,[22] has been discussed previously,[23,24] utilized synthetically,[25] and investigated theoretically.[26]

Received: August 25, 2018
Published: September 21, 2018

DOI: 10.1021/jacs.8b09174
J. Am. Chem. Soc. 2018, 140, 13478−13487

Scheme 1. Synthesis of (*S*)-CTTV[a,b]

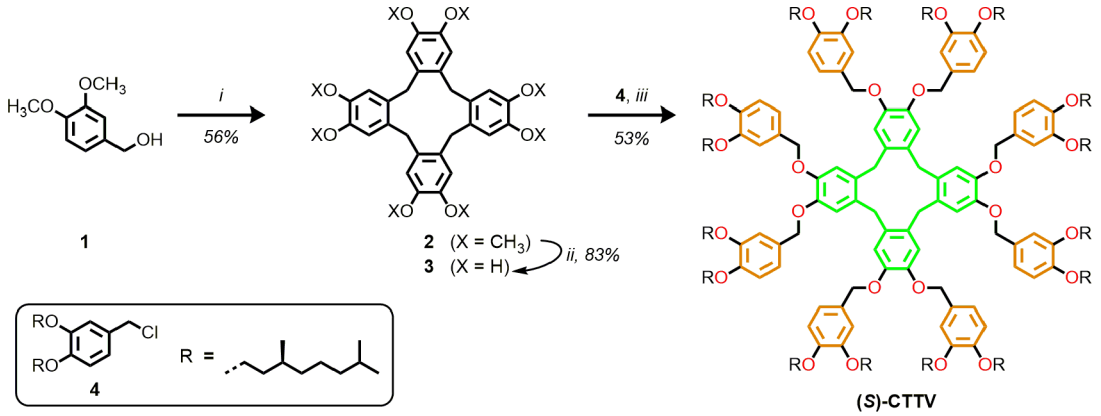

[a]Reagents and conditions: (*i*) CF_3COOH, CH_2Cl_2, 0 °C, 4 h; (*ii*) BBr_3, CH_2Cl_2, reflux, 2 h; (*iii*) K_2CO_3, DMF, 80 °C, 16 h. [b]Color code of (*S*)-CTTV: CTTV core, green; phenyl rings of dendrons, orange; O atoms, red; other atoms, black.

The conformation, or secondary structure, of a molecule determines whether self-assembly proceeds to give columnar or spherical tertiary structures, which have so far been considered mutually exclusive.[1j,l] Hence the assembly of supramolecular spheres into supramolecular columns is not expected and was only recently reported.[27] Spherical objects such as gold nanoparticles[28] or C_{60} fullerenes[29] have been embedded within supramolecular columns, but the supramolecular structure is dictated in these cases by the conformation of dendrons jacketing the spherical core. The supramolecular columns cannot be considered as an assembly of isolated nanoparticles or fullerenes, but rather as spherical objects (nanoparticles or fullerenes) suspended in an otherwise columnar assembly of dendrons.

Recently a supramolecular column assembled from supramolecular spherical objects was proposed for a perylene bisimide (PBI) dendronized with two second-generation self-assembling benzyl ether dendrons, G2-PBI.[27] G2-PBI organized into a 2D columnar hexagonal phase with intracolumnar order (Φ_h^{io1}) comprising supramolecular columns of stacked molecular crowns, a BCC phase comprising supramolecular spheres, and an intermediate columnar phase between the Φ_h^{io1} and BCC phases. It was proposed that the supramolecular columns of this intermediate columnar phase were constructed from supramolecular spheres as a means of transitioning between the columnar and cubic phases,[27a] mediated by the flexibility of the molecular crown-like conformation and consistent with a proposed "pinching off" mechanism for the column-to-sphere transition.[30]

Although transitions between columnar and cubic phases have been observed in multiple crown-like dendronized molecules, including cyclotriveratrylenes (CTV)[6a] and triphenylenes (Tp),[6b] no other column-from-spheres structure has been encountered. Crown-like CTV molecules generate pyramidal columns,[31] helical columns,[6,32] and cubic phases self-organized from supramolecular spheres.[6a,32b] Their periodic arrays exhibit supramolecular deracemization in the bulk state[6c] via crown inversion[33] and supramolecular orientational memory upon transition between columnar and cubic phases.[32b] In contrast to CTV, cyclotetraveratrylene (CTTV)[34] has a much less rigid core, which can access multiple conformations, among which the crown is energetically unstable.[34c]

In this publication, a columnar phase in which supramolecular columns are constructed from supramolecular spheres independently of the presence of a cubic phase is reported. A CTTV derivative dendronized with eight chiral minidendrons, discovered by screening a library of dendronized CTTV derivatives, self-assembles into supramolecular columns comprising stacked disc-like molecules. Upon heating, a first-order phase transition occurs to generate a distinct columnar phase in which molecules self-assemble into supramolecular spheres within the supramolecular columns. Circular dichroism spectroscopy demonstrates that these supramolecular spheres are chiral, and this chirality was exploited to monitor the column to column-from-spheres transition. Notably, further heating does not provide a cubic phase, but instead results in an isotropic melt. The column-from-spheres structure independent of subsequent transition to a 3D phase generated from spheres represents a new mechanism for the self-organization of supramolecular columns.

RESULTS AND DISCUSSION

Synthesis of Cyclotetraveratrylene with Chiral Minidendrons, (*S*)-CTTV. (*S*)-(3,4)dm8*G1-CTTV (hereafter "(*S*)-CTTV") was discovered by screening a library of CTTV derivatives dendronized with a variety of chiral and achiral first- and second-generation dendrons (Supporting Scheme 1). The columns-from-spheres structure was observed only for (*S*)-CTTV. It is not known why other dendronized CTTVs do not exhibit this structure. The chiral first-generation minidendron attached to (*S*)-CTTV was previously exploited in a CTV derivative that exhibited deracemization of its homochiral columns in its crystalline bulk state.[6c] The synthesis of (*S*)-CTTV is summarized in Scheme 1.

The CTTV core was prepared by cyclooligomerization[35] of veratryl alcohol **1** in trifluoroacetic acid and dichloromethane at 0 °C for 4 h. The choice of acid and concentration of reagents had been previously optimized to favor the tetrameric product **2**,[35a] which was isolated after recrystallization from a mixture of chloroform and benzene (8:3 v/v) in 56% yield. Demethylation of **2** with boron tribromide in dichloromethane at reflux for 2 h gave $CTTV(OH)_8$ (**3**)[34b] in 83% yield after recrystallization from aqueous ethanol. Williamson etherification of **3** with chiral minidendron **4**, which was prepared as reported previously,[6a] proceeded in 16 h at 80 °C in

DOI: 10.1021/jacs.8b09174
J. Am. Chem. Soc. 2018, 140, 13478−13487

dimethylformamide (DMF) with K_2CO_3 as base. Purification by column chromatography and recrystallization from acetone gave analytically pure (*S*)-CTTV in 53% isolated yield.

Thermal Analysis by Differential Scanning Calorimetry. The thermal phase behavior of (*S*)-CTTV was analyzed by differential scanning calorimetry (DSC, Figure 1). Phases

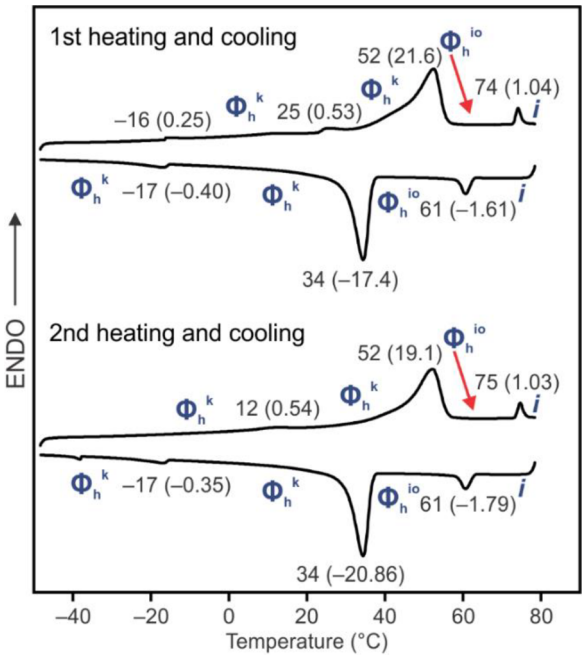

Figure 1. DSC traces of (*S*)-CTTV upon (top) first heating and cooling and (bottom) second heating and cooling, at a rate of 10 °C/min. Phases determined in XRD (defined in main text), transition temperatures (in °C), and associated enthalpy changes (in parentheses, in kcal/mol) are indicated.

indicated in Figure 1 were determined by X-ray diffraction (XRD) experiments, to be discussed later. The as-prepared sample of (*S*)-CTTV exhibits a 3D crystalline columnar hexagonal phase (Φ_h^k) at room temperature (23 °C). At 52 °C on first heating at 10 °C/min, the Φ_h^k phase transitions into a 2D columnar hexagonal phase with intracolumnar order (Φ_h^{io}). This phase is stable until isotropization at 74 °C, above which an isotropic melt is observed. Upon first cooling, the same sequence of phases is observed with moderate supercooling: the Φ_h^{io} and Φ_h^k phases are re-formed at 61 and 34 °C, respectively. The low-enthalpy transitions at −16 and 25 °C upon first heating and −17 °C upon first cooling are accompanied by small changes in the relative intensity of XRD peaks, corresponding to a limited degree of crystallization of the aliphatic chains of (*S*)-CTTV on cooling and their melting on heating. Subsequent heating and cooling cycles reproduce the thermal behavior observed upon first heating and cooling. Structural analysis parameters are summarized in Table 1.

Supramolecular Columns Self-Organized from Conformationally Flexible Disc-like Molecules. XRD analysis of an oriented fiber of (*S*)-CTTV in the Φ_h^k and Φ_h^{io} phases and accompanying models generated via structural and retrostructural analysis are shown in Figures 2 and 3.

XRD measurements were taken at two sample-to-detector distances: 0.54 m (denoted intermediate-angle X-ray scattering, IAXS) and 0.07 m (denoted wide-angle X-ray scattering, WAXS), to examine different length scales in the supramolecular assemblies of (*S*)-CTTV. IAXS data of the Φ_h^k phase (Figure 2a) probe intercolumnar packing of supramolecular columns into an array and are consistent with a hexagonal array with column diameter D_{col} (= a) of 36.0 Å (Table 1 and Supporting Figure 1). In contrast, WAXS provides information about the intracolumnar packing of molecules (Figure 2b) and suggests that the stratum thickness within the supramolecular column is 5.5 Å. This thickness can be combined with the experimental density (1.01 g/cm^3) to calculate the number of molecules per stratum of the column, μ = 1.01; that is, a single molecule of (*S*)-CTTV forms a complete disc within the supramolecular column. Tilt features in the WAXS pattern (Figure 2b, blue ellipses, and Figure 2c) indicate that the dendrons of (*S*)-CTTV are tilted by 30° with respect to the column axis, consistent with a crown-like conformation of the molecule (Figure 2d). The supramolecular column (Figure 2e) is thus composed of single molecules of (*S*)-CTTV with tilted dendrons, stacked atop each other to give a supramolecular column that is helical (Figure 2e−h), as evidenced by CD, to be discussed later. These columns self-organize in turn into a columnar hexagonal array.

Supramolecular Columns Assembled from Supramolecular Spheres: The Column-from-Spheres Model. Although the equatorial WAXS data of the Φ_h^{io} phase (Figure 3b) are also consistent with a columnar hexagonal array (Supporting Figure 1), there are substantial differences between the patterns of the Φ_h^{io} phase and those of the Φ_h^k phase (Figure 2b). No tilt or meridional features are apparent, and instead six features with low q values (i.e., close to the center) are observed. An azimuthal plot (Figure 3d) of these features (labeled 1 to 6 in Figure 3a−c) suggests that they appear at ∼60° intervals and that there are two distinct classes of features: features 1 and 4 are sharp, intense, equatorial peaks (q = 0.218 Å^{-1}), whereas features 2, 3, 5, and 6 are broad, diffuse, off-axis maxima (q = 0.221 Å^{-1}). This pattern of

Table 1. Structural Analysis of (*S*)-CTTV by XRD

T (°C)	phase[a]	a, b, c (Å)[b]	T (Å)[c]	P (g/cm^3)	M_{wt} (g/mol)[d]	μ[e]	D_{col} (Å)[f]	d_{100}, d_{110}, d_{200}, d_{210}, d_{300} (Å)[g]
15	Φ_h^k	36.0, 36.0, 44.0	5.5	1.01[h]	3709.8	1.0	36.0	31.2, 18.0, 15.6,11.8, 10.4
60	Φ_h^{io}	34.4, 34.4, –	–	0.98[i]		5.6	34.4[j]	29.8, 17.2, 14.9, 11.3, 9.5

[a]Phase notation: Φ_h^k, 3D crystalline columnar hexagonal phase; Φ_h^{io}, 2D liquid crystalline columnar hexagonal phase with intracolumnar order. [b]Lattice parameters calculated using $d_{hk0} = (\sqrt{3}a/2)(h^2 + k^2 + hk)^{-1/2}$. [c]Average column stratum thickness calculated from the meridional axis features of WAXS fiber patterns. [d]Molecular weight. [e]Average number of dendrimers forming the supramolecular object calculated using $\mu = (N_A A t \rho)(M_{wt})^{-1}$ where $N_A = 6.022 \times 10^{23}$ mol^{-1} = Avogadro's number and A is the area of the column cross-section calculated from the lattice parameters. In the Φ_h^k phase, μ defines the number of dendrimers in a column stratum with thickness t. In the Φ_h^{io} phase, μ defines the number of dendrimers in a supramolecular sphere occupying a length of the column equal to the sphere diameter, i.e., with thickness $t = a$. [f]Column diameter ($D_{col} = a$). [g]Experimental d-spacings for the Φ_h phases. [h]Experimental density measured at 23 °C. [i]Experimental density measured at 23 °C after quenching from 60 °C into liquid N_2, and calculated density (details in Supporting Information). [j]Diameter of column = diameter of sphere.

DOI: 10.1021/jacs.8b09174
J. Am. Chem. Soc. 2018, 140, 13478−13487

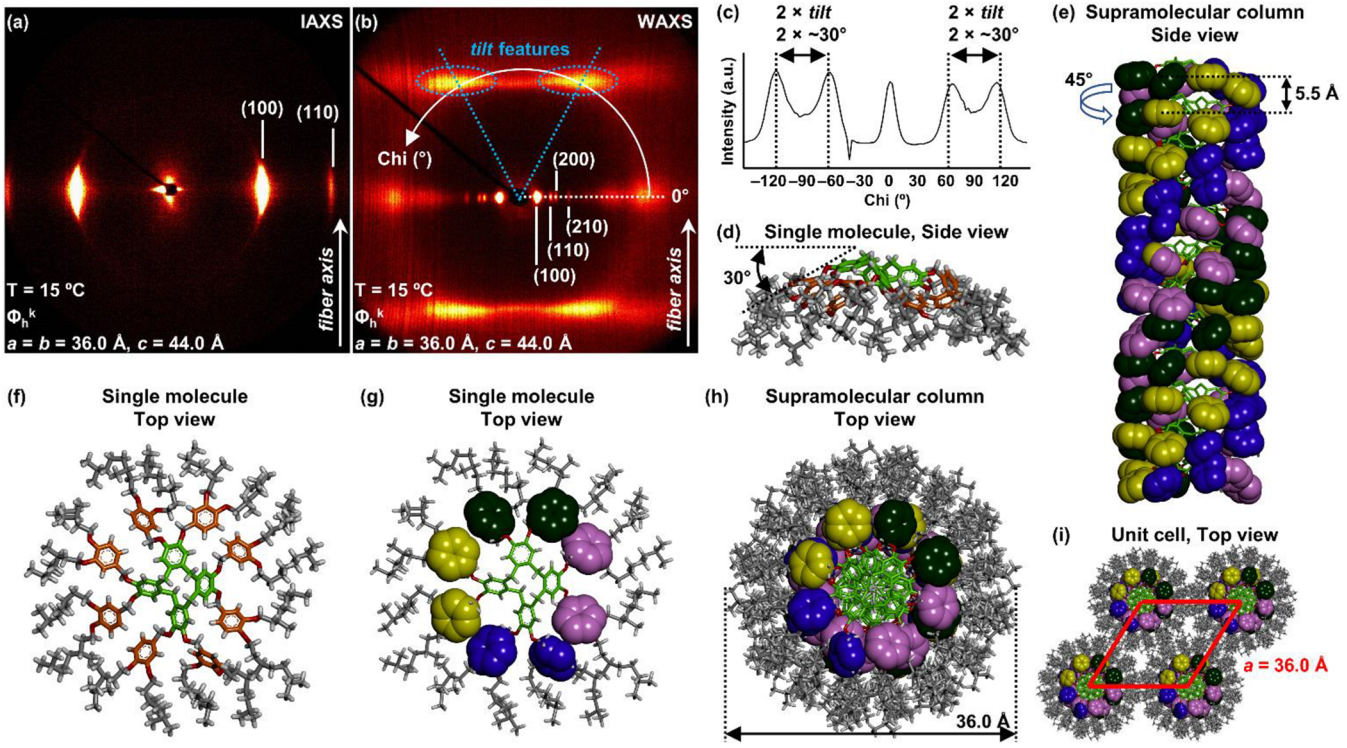

Figure 2. XRD patterns and molecular models of the 3D crystalline columnar hexagonal (Φ_h^k) phase of (*S*)-CTTV generated from tilted crowns. (a, b) Experimental XRD patterns collected with a sample-to-detector distance of (a) 0.54 m (IAXS) and (b) 0.07 m (WAXS). Temperature, phase, lattice parameters, and fiber axis are indicated. (c) Azimuthal plot of tilt features in (b). (d–i) Molecular models of the Φ_h^k phase: (d) single molecule, side view; (e) supramolecular column, side view, with alkyl chains omitted for clarity; (f, g) single molecule, top view; (h) supramolecular column, top view; (i) unit cell, top view. Color code: O, red; C atoms of the CTTV core, green; C atoms of phenyl rings, orange; C atoms of the peripheral alkyl chains, gray; H, white; dendron phenyl rings shown as colored CPK representations in (e) and (g)–(i).

features is consistent with the XRD data of the column-from-spheres model proposed for the intermediate Φ_h^{io2} phase in a G2-PBI.[27a] An estimate of the correlation length of the diffuse features in Figure 3a was calculated using the Scherrer equation ($\xi \approx 2\pi$/fwhm, where fwhm = full-width at half-maximum) to be ~95 Å, that is, on the order of two or three supramolecular spheres.

Taking the diameter of the supramolecular sphere to be equal to D_{col} (34.4 Å) and the density of the Φ_h^{io} phase (0.98 g/cm^3) suggest that there are six molecules in the supramolecular sphere. Measurement of density via the flotation method at higher temperature was unreliable due to convection flow and thermal gradients at elevated temperature. Instead the density of the Φ_h^{io} phase was determined by two methods: by measuring at 23 °C the density of a fiber that was heated to 60 °C and subsequently quenched in liquid N_2 and by calculation,[37] accounting for the thermal expansion of the aliphatic portion of (*S*)-CTTV (see Supporting Information for details).[38] Both values provided a density of 0.98 g/cm^3, from which we calculate that there are 5.6, i.e., ~6, molecules per supramolecular sphere. The disparity between 5.6 and 6 is accounted for by experimental uncertainties in the determination of lattice parameters by XRD and density. A value of six CTTV molecules per sphere is consistent with CTV (μ = 3.3–4.5, D_{col} = 33.8–45.9 Å)[6a] and triphenylene (μ = 5.0–8.4, D_{col} = 40.1–67.3 Å)[6b] derivatives dendronized with first-generation dendrons previously reported to form supramolecular spheres. A model of the supramolecular columns-from-spheres of (*S*)-CTTV with *P6mm* symmetry is presented in Figure 3e–h. Note that in Figure 3h the supramolecular spheres are depicted as non-space-filling to aid visualization, analogous to typical depictions of other phases generated from spheres such as cubic phases.[36] In practice, supramolecular spheres will be in contact such that the peripheral alkyl chains form a continuous domain throughout the structure and there is no space between spheres. Consistent with dendronized CTV[6a] and triphenylenes,[6b] the supramolecular sphere is a supramolecular spherical assembly of (*S*)-CTTV constructed from a short spherically distorted fragment of its helical supramolecular column. This fragment contains on average six molecules, as determined by density calculations (Table 1), and exhibits chirality dictated by the helical arrangement of molecules within the spherical helix assembly (Supporting Figure 2) and evidenced by circular dichroism (CD) spectroscopy, to be discussed later.

In the proposed model, supramolecular spherical objects are randomly rotationally disordered within the supramolecular column, with spheres in adjacent columns longitudinally displaced along the column axis by approximately z = 0, c/3, and 2c/3, respectively (Figures 3h and 4). A numerical simulation of the diffraction of a column-from-spheres model was performed, in which solid spheres are displaced along the columns of a columnar hexagonal array by exactly z = 0, c/3, and 2c/3, respectively (Figure 3c).[27a] A columnar hexagonal array of supramolecular spheres with exactly these displacements is equivalent to a BCC phase,[27a] where the body diagonal of the BCC unit cell (=$\sqrt{3}a$) is equal to twice the diameter of the supramolecular sphere, D_{sph}. Hence $a = (2/\sqrt{3})D_{sph}$, and therefore the Φ_h^{io} phase with D_{col} = 34.4 Å would be equivalent to a BCC phase with a = 39.7 Å. The

DOI: 10.1021/jacs.8b09174
J. Am. Chem. Soc. 2018, 140, 13478–13487

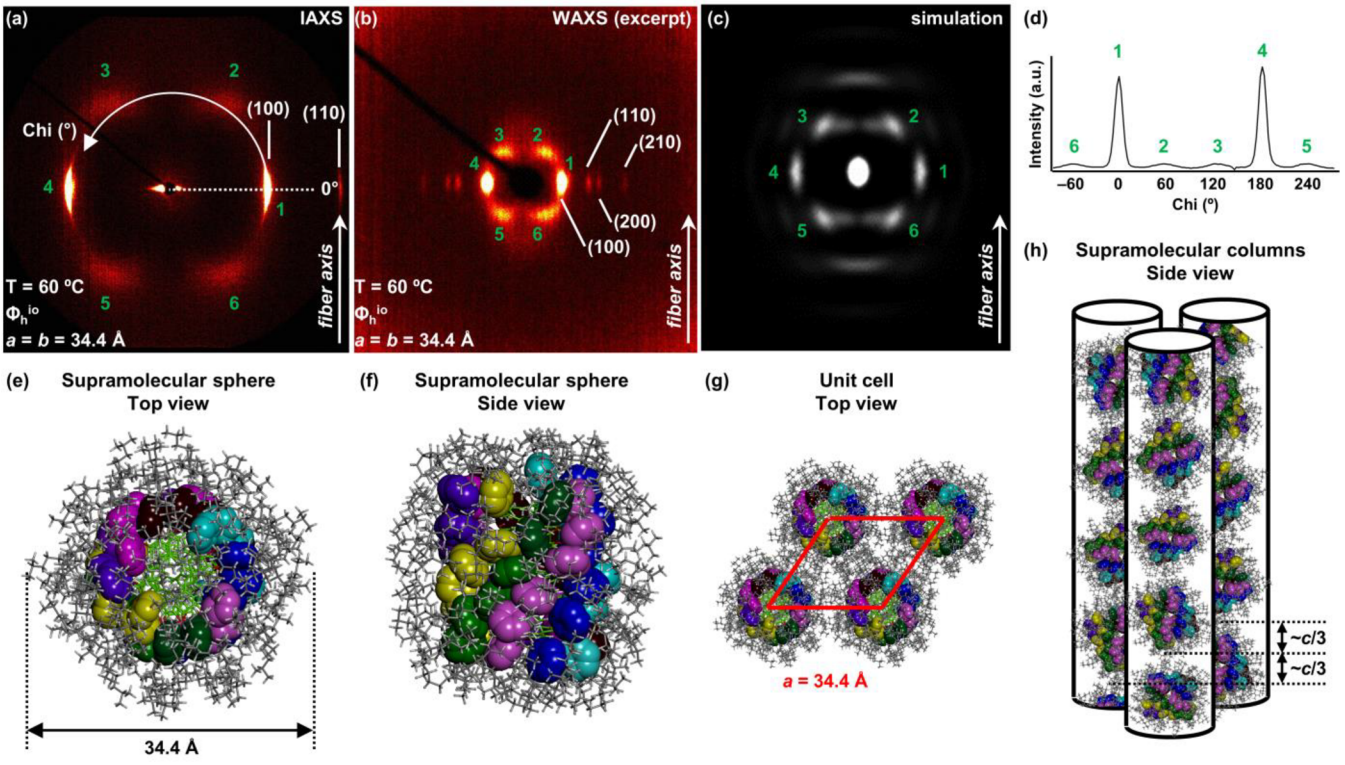

Figure 3. XRD patterns and molecular models of the 2D liquid crystalline columnar hexagonal phase with intracolumnar order (Φ_h^{io}) of (*S*)-CTTV generated from supramolecular spheres. (a, b) Experimental XRD patterns collected with a sample-to-detector distance of (a) 0.54 m (IAXS) and (b) 0.07 m (WAXS). Temperature, phase, lattice parameters, and fiber axis are indicated. (c) Numerical simulation of a hexagonal array of columns constructed from supramolecular spheres.[27a] (d) Azimuthal plot of features 1 to 6 in (a). (e–h) Molecular models of the Φ_h^{io} phase: supramolecular sphere, (e) top and (f) side view; (g) unit cell, top view; (h) supramolecular columns, side view. Spheres are depicted as non-space-filling to aid visualization.[36] Color code: O, red; N, blue; C atoms of the CTTV core, green; C atoms of the peripheral alkyl chains, gray; H, white; dendron phenyl rings shown as colored CPK representations.

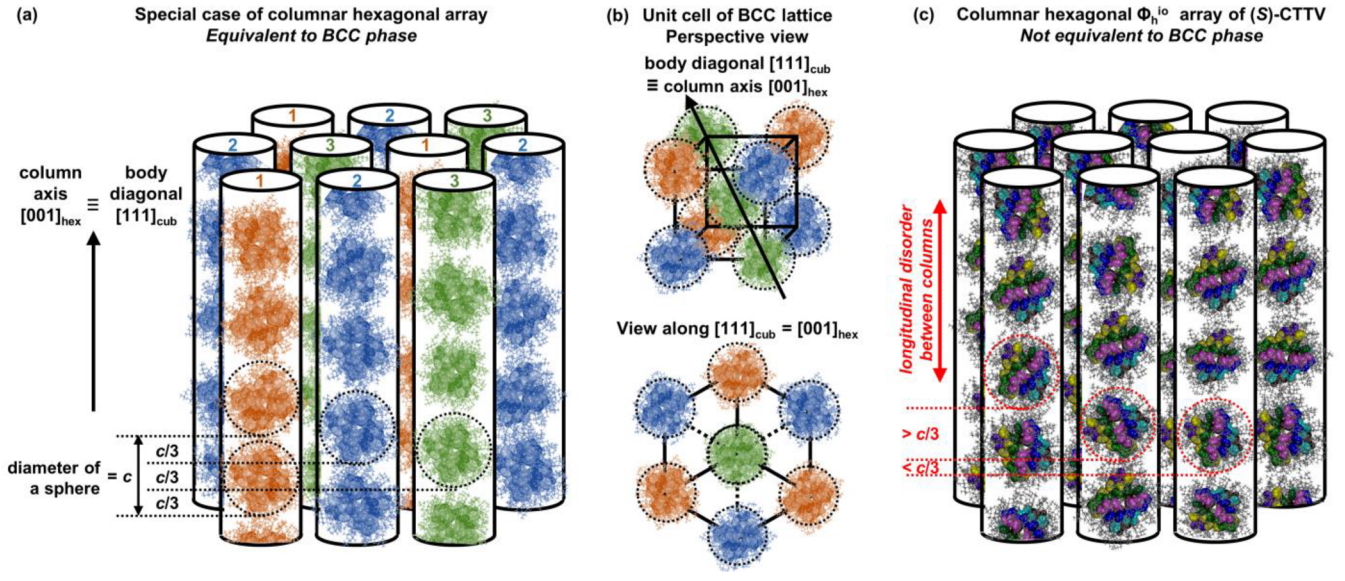

Figure 4. Comparison of column-from-spheres models. (a) A body centered cubic (BCC) lattice can be treated as a $\sqrt{3} \times \sqrt{3}$ hexagonal lattice comprising three types of columns in which supramolecular spheres are displaced along the column axis by $z = 0$, $z = c/3$, and $z = 2c/3$, respectively. (b) Unit cell of equivalent BCC lattice. (c) In the column-from-spheres model proposed for the Φ_h^{io} phase of (*S*)-CTTV, longitudinal disorder of the supramolecular spheres along the column axis reduces the symmetry of the periodic array so that it is not equivalent to a BCC phase. Spheres are depicted as non-space-filling to aid visualization.[36]

positions of diffraction features arising from this numerical simulation (Figure 3c) are consistent with the experimental data (Figure 3a), but the simulated pattern overestimates the intensity and sharpness of features 2, 3, 5, and 6 as well as a meridional feature at a higher q value. Disorder in the displacement of supramolecular spheres along the column axis

DOI: 10.1021/jacs.8b09174
J. Am. Chem. Soc. 2018, 140, 13478–13487

eliminates the cubic symmetry of the array, which is supported by the diffuse nature of features 2, 3, 5, and 6 (Figure 3a). The meridional feature in the numerical simulation (Figure 3c) is manifested as a very diffuse region of diffraction on the meridian in the experimental pattern (Figure 3b). Hence the column-from-spheres model proposes supramolecular columns comprising supramolecular spheres that are translationally disordered along the column axis and rotationally disordered and is therefore most appropriately described as a Φ_h^{io} phase. This assignment is supported also by the observation of (*hk*0) peaks consistent with a hexagonal lattice (Figure 3b and Supporting Figure 1).

The assignment of the Φ_h^{io} phase as a columnar array in which supramolecular columns comprise supramolecular spheres is supported by modeling and simulation (Figure 5).

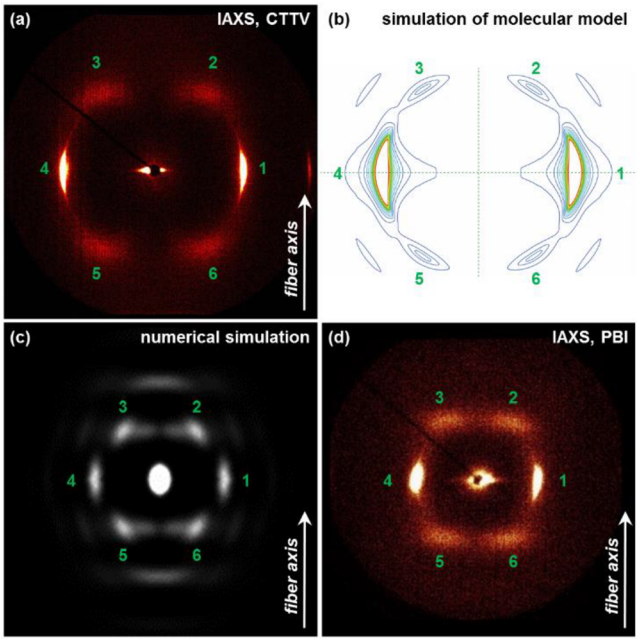

Figure 5. Experimental and simulated XRD patterns for hexagonal arrays of supramolecular columns constructed from supramolecular spheres. (a) Experimental XRD pattern of the Φ_h^{io} phase of (*S*)-CTTV. (b, c) XRD patterns of the Φ_h^{io} phase of (*S*)-CTTV simulated from (b) the molecular model depicted in Figure 3e–h and (c) a columnar hexagonal array of solid spheres displaced along the column axis.[27a] (d) Experimental XRD pattern of the Φ_h^{io2} phase of G2-PBI,[27a] in which supramolecular columns are constructed from supramolecular spheres.

A simulation of the XRD pattern expected from the molecular model presented in Figure 3e–h and described above agrees well with the experimentally observed XRD pattern (compare Figure 5a,b), in terms of both the positions of features and their relative intensities. Indeed, the weakest features at higher *q* in the simulation (Figure 5b) are too weak to be observed experimentally (Figure 5a). Additional simulation of a columnar hexagonal array of solid spheres longitudinally displaced along the column axis (Figure 5c) also reproduces the experimentally observed positions of features, but provides only moderate agreement for relative intensities as the model neglects the anisotropic distribution of electron density within the supramolecular sphere. The experimental XRD pattern of the Φ_h^{io} phase of (*S*)-CTTV (Figure 5a) shows substantial similarity to the experimental XRD pattern of G2-PBI (Figure 5d),[27a] with two bright peaks at positions 1 and 4 and four diffuse features at positions 2, 3, 5, and 6. The features of (*S*)-CTTV (Figure 5a) are located at higher *q* values than those of G2-PBI (Figure 5d) due to the smaller size of its supramolecular columns ($D_{col,CTTV}$ = 34.4 Å vs $D_{col,PBI}$ = 46.1 Å).

An alternative model to explain the diffuse features in Figure 3a,b could invoke a columnar arrangement of discs or pseudodiscs rather than a short-range intercolumnar order of spherical objects, to give undulating columns.[39] However, undulating columns would be expected to give rise to a relatively strong diffraction feature between 3.5 and 6.0 Å, corresponding to the distance between column strata. This is absent from the experimental XRD of the Φ_h^{io} phase (Figure 3b), due to the formation of smaller helical stacks along the column axis, consistent with the formation of supramolecular spherical objects that are rotationally disordered about the column axis. The diffuse nature of the features at positions 2, 3, 5, and 6 (Figure 3a) supports short-range intra- and intercolumnar order, whereas higher intracolumnar order, and a concomitantly sharper diffraction feature, would be expected within an array of undulating columns. Furthermore, the diffuse features at positions 2, 3, 5, and 6 in the diffraction patterns of both (*S*)-CTTV and G2-PBI have *q* values almost identical to the sharp features at positions 1 and 4. This supports the formation of distinct supramolecular spheres rather than undulated columns, which would give rise to sharp off-axis features at positions 2, 3, 5, and 6, at higher *q* values.[40]

Another alternative explanation for the observation of an apparent column-from-spheres model is coexistence of Φ_h and BCC phases, which would result from a slow transition between the two phases.[41] Diffraction features from both the Φ_h and BCC phases would be observed by XRD, and hence broad features 2, 3, 5, and 6 in Figure 5a would have to be attributed to the (110) features of a BCC array. In this case, a similarly broad ($1\bar{3}0$) feature of the BCC phase would be expected approximately at positions 1 and 4 in Figure 5a. However, these broad features are not observed, and instead only sharp diffraction peaks, consistent with the (100) peak of a Φ_h phase, are observed. Furthermore, DSC demonstrates a large enthalpy transition between the Φ_h^{k} and Φ_h^{io} phases (Figure 1), indicative of a distinct phase transition rather than a broad range of coexistence. During this transition, the benzyl ether dendrons attached to the CTTV core exhibit increased thermal motion. The curvature of the dendrons increases, driving crown–crown inversion. This inversion generates crowns and inverted crowns (Figure 3f) rather than all crowns within a column pointing in the same direction (Figure 2d) and drives the formation of supramolecular spheres.

In summary, DSC, XRD, molecular modeling, and simulation of XRD favor a columns-from-spheres model rather than alternative explanations such as an array of undulated columns or coexistence of Φ_h and BCC phases. Attempts to visualize the spheres within the columns-from-spheres via atomic force microscopy (AFM) have not yet succeeded, as discriminating the boundaries of individual spheres is approaching the limit of the resolution of AFM and other real-space imaging techniques such as transmission electron microscopy.[15a]

Propagation of Supramolecular Chirality from Columns to Columns-from-Spheres. Chiral supramolecular structures arise from the self-assembly of both chiral and achiral building blocks.[42] The self-assembly of a chiral building block generates a homochiral supramolecular assembly by

DOI: 10.1021/jacs.8b09174
J. Am. Chem. Soc. 2018, 140, 13478–13487

selecting the handedness of an already chiral structure,[6,10,11,43,44] and thus it was expected that self-assembly of homochiral (*S*)-CTTV would generate homochiral supramolecular columns. The proposed column-from-spheres model of (*S*)-CTTV describes the supramolecular sphere as a short, spherically distorted fragment of the supramolecular column (Figure 3 and Supporting Figure 2), consistent with previous studies on supramolecular spheres from CTV and triphenylene.[6] In those studies, the helical structure of the supramolecular sphere was confirmed by CD spectroscopy.

Hence a spin-coated film of (*S*)-CTTV was monitored using CD as a function of temperature to ascertain how phase transitions affect the homochiral assembly of (*S*)-CTTV (Figure 6). There are three distinct regimes identifiable by

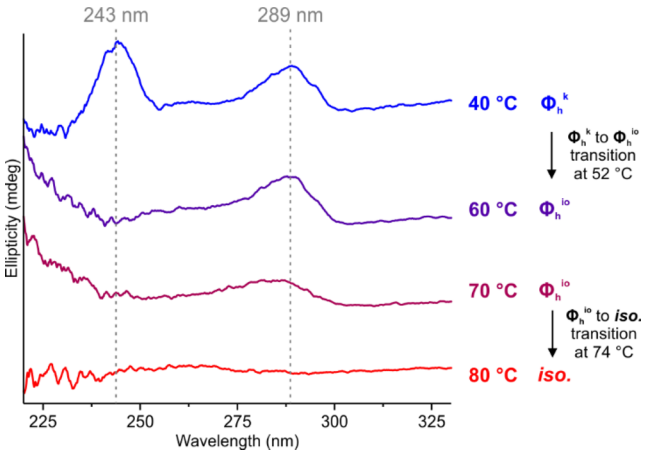

Figure 6. Temperature dependence of the CD spectrum of a spin-coated film of (*S*)-CTTV cast from $CHCl_3$ (2% w/v). Phases and transition temperatures determined by XRD and DSC are indicated. Spectra recorded at different temperatures are vertically shifted for clarity.

CD. In the Φ_h^k phase, the long-range helical order in the supramolecular column provides the strongest CD signal, with two discernible features at 243 and 289 nm. Upon heating above the Φ_h^k-to-Φ_h^{io} phase transition (52 °C), the feature at 243 nm disappears, and only the CD feature at 289 nm remains. Cooling the film reproduces the same sequence of CD spectra (Supporting Figure 3), although the feature at ∼240 nm at 25 °C has negative ellipticity. This difference may arise because the Φ_h^k phase measured upon heating is the as-prepared sample, whereas the Φ_h^k phase measured upon cooling is generated by slow cooling from the isotropic phase. This is indicative of a shorter range helical order, as would be expected from distinct supramolecular spheres comprising only six molecules in a continuous molecular stack. Further heating reduces the intensity of the feature at 289 nm until, in the isotropic melt (above 74 °C), no CD features are observed. These data support extended helical order in the columnar Φ_h^k phase and a disruption to the extent of that helical order in the column-from-spheres Φ_h^{io} phase. The presence of a CD signal in the Φ_h^{io} phase suggests lower range helical order, as expected from the relatively short molecular stacks which constitute the supramolecular spheres, but evidence that there must be some helical order present in the Φ_h^{io} phase. Therefore, the evolution of the CD of (*S*)-CTTV as a function of temperature is consistent with a column-from-spheres model in the Φ_h^{io} array of (*S*)-CTTV.

CONCLUSIONS

The structural and retrostructural analysis of a dendronized cyclotetraveratrylene derivative, (*S*)-CTTV, has uncovered a columnar array in which supramolecular columns are constructed from supramolecular spheres. This structure represents a new mechanism to self-organize supramolecular columns that complements and expands upon existing frameworks for the assembly of soft matter.[45] Whereas this column-from-spheres model had been previously invoked for an intermediate phase between a columnar phase comprising stacked crowns and a body-centered cubic phase comprising supramolecular spheres,[27] the column-from-spheres structure observed for (*S*)-CTTV exists as a standalone phase without subsequent transition to a cubic array. The lack of a cubic phase is consistent with the self-assembly of a CTV dendronized with the same minidendron,[6a,c] which also assembled into only columnar phases. However, it remains to be clarified why (*S*)-CTTV forms this intermediate column-from-spheres structure yet is unable to transition to a 3D phase generated from supramolecular spheres.

The supramolecular chirality of (*S*)-CTTV in the columnar Φ_h^k phase was maintained in the column-from-spheres Φ_h^{io} phase, albeit with lower magnitude as expected from the shorter correlation length of helical molecular stacks. This result reinforces previous observations that supramolecular spheres assembled from crown- and disc-like molecules are chiral.[6,44] Previous work has also shown that spheres assembled from conical molecules are chiral,[11,46] although this has yet to be generalized.

The column-from-spheres phase previously observed as an intermediate phase between a columnar and a BCC phase was implicated in the mechanism of supramolecular orientational memory,[27b] a phenomenon that results in reorientation of columnar domains during heating to and cooling from a cubic phase of supramolecular spheres.[27b,32b] The demonstration here that spheres in the column-from-spheres model are chiral raises the question of how chirality is propagated and transferred during supramolecular orientational memory.[27b,32b] This question and the generality of columnar arrays constructed from supramolecular spheres in soft matter are under investigation.

ASSOCIATED CONTENT

Supporting Information

The Supporting Information is available free of charge on the ACS Publications website at DOI: 10.1021/jacs.8b09174.

Synthetic procedures with complete characterization data, experimental methods, and structural analysis parameters (PDF)

AUTHOR INFORMATION

Corresponding Author

*percec@sas.upenn.edu

ORCID

Mohammad R. Imam: 0000-0003-0794-3725
Mihai Peterca: 0000-0002-7247-4008
Benjamin E. Partridge: 0000-0003-2359-1280
Daniela A. Wilson: 0000-0002-8796-2274
Goran Ungar: 0000-0002-9743-2656
Virgil Percec: 0000-0001-5926-0489

DOI: 10.1021/jacs.8b09174
J. Am. Chem. Soc. 2018, 140, 13478−13487

Present Addresses

[⊥]D.S.: Department of Chemistry, Stony Brook University, Stony Brook, New York 11794, United States.

[¶]M.R.I.: Department of Chemistry, King Fahd University of Petroleum and Minerals (KFUPM), Dhahran, Kingdom of Saudi Arabia.

[#]D.A.W.: Institute for Molecules and Materials, Radboud University, Heyendaalseweg 135, 6525 AJ, Nijmegen, The Netherlands.

Notes

The authors declare no competing financial interest.

■ ACKNOWLEDGMENTS

Financial support by the National Science Foundation (DMR-1066116 and DMR-1807127 (V.P.), DMR-1120901 (V.P. and P.A.H.)), the Humboldt Foundation (V.P.), and the P. Roy Vagelos Chair at Penn (V.P.) is gratefully acknowledged. B.E.P. thanks the Howard Hughes Medical Institute for an International Student Research Fellowship.

■ REFERENCES

(1) (a) Chandrasekhar, S.; Sadashiva, B. K.; Suresh, K. A. Liquid Crystals of Disc-like Molecules. *Pramana* **1977**, *9*, 471−480. (b) Billard, J.; Dubois, J. C.; Nyugen, H. T.; Zann, A. Mesophase of Disc-like Molecules. *Nouv. J. Chem.* **1978**, *2*, 535−540. (c) Levelut, A. M. Structure of a Disk-like Mesophase. *J. Phys., Lett.* **1979**, *40*, L81−L84. (d) Fréchet, J. M. J. Functional Polymers and Dendrimers − Reactivity, Molecular Architecture, and Interfacial Energy. *Science* **1994**, *263*, 1710−1715. (e) Hill, D. J.; Mio, M. J.; Prince, R. B.; Hughes, T. S.; Moore, J. S. A Field Guide to Foldamers. *Chem. Rev.* **2001**, *101*, 3893−4012. (f) Bushby, R. J.; Lozman, O. R. Discotic Liquid Crystals 25 Years On. *Curr. Opin. Colloid Interface Sci.* **2002**, *7*, 343−354. (g) Kumar, S. Self-Organization of Disc-like Molecules: Chemical Aspects. *Chem. Soc. Rev.* **2006**, *35*, 83−109. (h) Laschat, S.; Baro, A.; Steinke, N.; Giesselmann, F.; Hägele, C.; Scalia, G.; Judele, R.; Kapatsina, E.; Sauer, S.; Schreivogel, A.; Tosoni, M. Discotic Liquid Crystals: From Tailor-Made Synthesis to Plastic Electronics. *Angew. Chem., Int. Ed.* **2007**, *46*, 4832−4887. (i) De Greef, T. F. A.; Smulders, M. M. J.; Wolffs, M.; Schenning, A. P. H. J.; Sijbesma, R. P.; Meijer, E. W. Supramolecular Polymerization. *Chem. Rev.* **2009**, *109*, 5687−5754. (j) Rosen, B. M.; Wilson, C. J.; Wilson, D. A.; Peterca, M.; Imam, M. R.; Percec, V. Dendron-Mediated Self-Assembly, Disassembly, and Self-Organization of Complex Systems. *Chem. Rev.* **2009**, *109*, 6275−6540. (k) Krieg, E.; Bastings, M. M. C.; Besenius, P.; Rybtchinski, B. Supramolecular Polymers in Aqueous Media. *Chem. Rev.* **2016**, *16*, 2414−2477. (l) Sun, H.-J.; Zhang, S.; Percec, V. From Structure to Function *via* Complex Supramolecular Dendrimer Systems. *Chem. Soc. Rev.* **2015**, *44*, 3900−3923. (m) Wöhrle, T.; Wurzbach, I.; Kirres, J.; Kostidou, A.; Kapernaum, N.; Litterscheidt, J.; Haenle, J. C.; Staffeld, P.; Baro, A.; Giesselmann, F.; Laschat, S. Discotic Liquid Crystals. *Chem. Rev.* **2016**, *116*, 1139−1241.

(2) (a) Percec, V.; Heck, J.; Lee, M.; Ungar, G.; Alvarez-Castillo, A. Poly{2-Vinyloxyethyl 3,4,5-Tris[4-(*n*-Dodecanyloxy)Benzyloxy]-Benzoate}: A Self-Assembled Supramolecular Polymer Similar to Tobacco Mosaic Virus. *J. Mater. Chem.* **1992**, *2*, 1033−1039. (b) Percec, V.; Johansson, G.; Ungar, G.; Zhou, J. Fluorophobic Effect Induces the Self-Assembly of Semifluorinated Tapered Monodendrons Containing Crown Ethers into Supramolecular Columnar Dendrimers Which Exhibit a Homeotropic Hexagonal Columnar Liquid Crystalline Phase. *J. Am. Chem. Soc.* **1996**, *118*, 9855−9866. (c) Percec, V.; Holerca, M. N.; Uchida, S.; Yeardley, D. J.; Ungar, G. Poly(Oxazoline)s with Tapered Minidendritic Side Groups as Models for the Design of Synthetic Macromolecules with Tertiary Structure. A Demonstration of the Limitations of Living Polymerization in the Design of 3-D Structures Based on Single Polymer Chain. *Biomacromolecules* **2001**, *2*, 729−740.

(3) (a) Ungar, G.; Abramic, D.; Percec, V.; Heck, J. A. Self-Assembly of Twin Tapered Bisamides into Supramolecular Columns Exhibiting Hexagonal Columnar Mesophases. Structural Evidence for a Microsegregated Model of the Supramolecular Column. *Liq. Cryst.* **1996**, *21*, 73−86. (b) Percec, V.; Bera, T. K.; Glodde, M.; Fu, Q.; Balagurusamy, V. S. K.; Heiney, P. A. Hierarchical Self-Assembly, Coassembly, and Self-Organization of Novel Liquid Crystalline Lattices and Superlattices from a Twin-Tapered Dendritic Benzamide and Its Four-Cylinder-Bundle Supramolecular Polymer. *Chem. - Eur. J.* **2003**, *9*, 921−935. (c) Percec, V.; Rudick, J. G.; Peterca, M.; Yurchenko, M. E.; Smidrkal, J.; Heiney, P. A. Supramolecular Structural Diversity Among First-Generation Hybrid Dendrimers and Twin Dendrons. *Chem. - Eur. J.* **2008**, *14*, 3355−3362.

(4) (a) Percec, V.; Imam, M. R.; Bera, T. K.; Balagurusamy, V. S. K.; Peterca, M.; Heiney, P. A. Self-Assembly of Semifluorinated Janus-Dendritic Benzamides into Bilayered Pyramidal Columns. *Angew. Chem., Int. Ed.* **2005**, *44*, 4739−4745. (b) Percec, V.; Imam, M. R.; Peterca, M.; Leowanawat, P. Self-Organizable Vesicular Columns Assembled from Polymers Dendronized with Semifluorinated Janus Dendrimers Act As Reverse Thermal Actuators. *J. Am. Chem. Soc.* **2012**, *134*, 4408−4420.

(5) (a) Percec, V.; Cho, W.-D.; Mosier, P. E.; Ungar, G.; Yeardley, D. J. P. Structural Analysis of Cylindrical and Spherical Supramolecular Dendrimers Quantifies the Concept of Monodendron Shape Control by Generation Number. *J. Am. Chem. Soc.* **1998**, *120*, 11061−11070. (b) Percec, V.; Cho, W. D.; Ungar, G. Increasing the Diameter of Cylindrical and Spherical Supramolecular Dendrimers by Decreasing the Solid Angle of Their Monodendrons *via* Periphery Functionalization. *J. Am. Chem. Soc.* **2000**, *122*, 10273−10281.

(6) (a) Percec, V.; Imam, M. R.; Peterca, M.; Wilson, D. A.; Heiney, P. A. Self-Assembly of Dendritic Crowns into Chiral Supramolecular Spheres. *J. Am. Chem. Soc.* **2009**, *131*, 1294−1304. (b) Percec, V.; Imam, M. R.; Peterca, M.; Wilson, D. A.; Graf, R.; Spiess, H. W.; Balagurusamy, V. S. K.; Heiney, P. A. Self-Assembly of Dendronized Triphenylenes into Helical Pyramidal Columns and Chiral Spheres. *J. Am. Chem. Soc.* **2009**, *131*, 7662−7677. (c) Roche, C.; Sun, H.-J.; Prendergast, M. E.; Leowanawat, P.; Partridge, B. E.; Heiney, P. A.; Araoka, F.; Graf, R.; Spiess, H. W.; Zeng, X.; Ungar, G.; Percec, V. Homochiral Columns Constructed by Chiral Self-Sorting During Supramolecular Helical Organization of Hat-Shaped Molecules. *J. Am. Chem. Soc.* **2014**, *136*, 7169−7185.

(7) (a) Leung, K. C. F.; Mendes, P. M.; Magonov, S. N.; Northrop, B. H.; Kim, S.; Patel, K.; Flood, A. H.; Tseng, H. R.; Stoddart, J. F. Supramolecular Self-Assembly of Dendronized Polymers: Reversible Control of the Polymer Architectures through Acid-Base Reactions. *J. Am. Chem. Soc.* **2006**, *128*, 10707−10715. (b) Prehm, M.; Liu, F.; Zeng, X.; Ungar, G.; Tschierske, C. Axial-Bundle Phases - New Modes of 2D, 3D, and Helical Columnar Self-Assembly in Liquid Crystalline Phases of Bolaamphiphiles with Swallow Tail Lateral Chains. *J. Am. Chem. Soc.* **2011**, *133*, 4906−4916. (c) Myśliwiec, D.; Donnio, B.; Chmielewski, P. J.; Heinrich, B.; Stepień, M. Peripherally Fused Porphyrins *via* the Scholl Reaction: Synthesis, Self-Assembly, and Mesomorphism. *J. Am. Chem. Soc.* **2012**, *134*, 4822−4833. (d) Shu, J.; Dudenko, D.; Esmaeili, M.; Park, J. H.; Punirredd, S. R.; Chang, J. Y.; Breiby, D. W.; Pisula, W.; Hansen, M. R. Coexistence of Helical Morphologies in Columnar Stacks of Star-Shaped Discotic Hydrazones. *J. Am. Chem. Soc.* **2013**, *135*, 11075−11086. (e) Yen, M. H.; Chaiprapa, J.; Zeng, X.; Liu, Y.; Cseh, L.; Mehl, G. H.; Ungar, G. Added Alkane Allows Thermal Thinning of Supramolecular Columns by Forming Superlattice-An X-Ray and Neutron Study. *J. Am. Chem. Soc.* **2016**, *138*, 5757−5760.

(8) (a) Percec, V.; Rudick, J. G.; Peterca, M.; Staley, S. R.; Wagner, M.; Obata, M.; Mitchell, C. M.; Cho, W. D.; Balagurusamy, V. S. K.; Lowe, J. N.; Glodde, M.; Weichold, O.; Chung, K. J.; Ghionni, N.; Magonov, S. N.; Heiney, P. A. Synthesis, Structural Analysis, and Visualization of a Library of Dendronized Polyphenylacetylenes. *Chem. - Eur. J.* **2006**, *12*, 5731−5746. (b) Percec, V.; Rudick, J. G.; Peterca, M.; Aqad, E.; Imam, M. R.; Heiney, P. A. Synthesis, Structural, and Retrostructural Analysis of Helical Dendronized

DOI: 10.1021/jacs.8b09174
J. Am. Chem. Soc. 2018, 140, 13478−13487

Poly(1-naphthylacetylene)s. *J. Polym. Sci., Part A: Polym. Chem.* **2007**, *45*, 4974−4987. (c) Tahar-Djebbar, I.; Nekelson, F.; Heinrich, B.; Donnio, B.; Guillon, D.; Kreher, D.; Mathevet, F.; Attias, A. J. Lamello-Columnar Mesophase Formation in a Side-Chain Liquid Crystal π-Conjugated Polymer Architecture. *Chem. Mater.* **2011**, *23*, 4653−4656. (d) Mu, B.; Li, Q.; Li, X.; Chen, J.; Fang, J.; Chen, D. Self-Assembled Helical Columnar Superstructures with Selective Homochirality. *Polym. Chem.* **2017**, *8*, 3457−3463. (e) Holerca, M. N.; Sahoo, D.; Peterca, M.; Partridge, B. E.; Heiney, P. A.; Percec, V. A Tetragonal Phase Self-Organized from Unimolecular Spheres Assembled from a Substituted Poly(2-Oxazoline). *Macromolecules* **2017**, *50*, 375−385.

(9) (a) Adam, D.; Schuhmacher, P.; Simmerer, J.; Häussling, L.; Siemensmeyer, K.; Etzbach, K. H.; Ringsdorf, H.; Haarer, D. Fast Photoconduction in the Highly Ordered Columnar Phase of a Discotic Liquid Crystal. *Nature* **1994**, *371*, 141−143. (b) Percec, V.; Glodde, M.; Bera, T. K.; Miura, Y.; Shiyanovskaya, I.; Singer, K. D.; Balagurusamy, V. S. K.; Heiney, P. A.; Schnell, I.; Rapp, A.; Spiess, H. W.; Hudson, S. D.; Duan, H. Self-Organization of Supramolecular Helical Dendrimers into Complex Electronic Materials. *Nature* **2002**, *419*, 384−387. (c) Idé, J.; Méreau, R.; Ducasse, L.; Castet, F.; Bock, H.; Olivier, Y.; Cornil, J.; Beljonne, D.; D'Avino, G.; Roscioni, O. M.; Muccioli, L.; Zannoni, C. Charge Dissociation at Interfaces between Discotic Liquid Crystals: The Surprising Role of Column Mismatch. *J. Am. Chem. Soc.* **2014**, *136*, 2911−2920. (d) Ho, M. S.; Partridge, B. E.; Sun, H. J.; Sahoo, D.; Leowanawat, P.; Peterca, M.; Graf, R.; Spiess, H. W.; Zeng, X.; Ungar, G.; Heiney, P. A.; Hsu, C.-S.; Percec, V. Screening Libraries of Semifluorinated Arylene Bisimides to Discover and Predict Thermodynamically Controlled Helical Crystallization. *ACS Comb. Sci.* **2016**, *18*, 723−739.

(10) (a) Percec, V.; Rudick, J. G.; Peterca, M.; Heiney, P. A. Nanomechanical Function from Self-Organizable Dendronized Helical Polyphenylacetylenes. *J. Am. Chem. Soc.* **2008**, *130*, 7503−7508. (b) Rudick, J. G.; Percec, V. Nanomechanical Function Made Possible by Suppressing Structural Transformations of Polyarylacetylenes. *Macromol. Chem. Phys.* **2008**, *209*, 1759−1768. (c) Andreopoulou, K. A.; Peterca, M.; Wilson, D. A.; Partridge, B. E.; Heiney, P. A.; Percec, V. Demonstrating the 8_1-Helicity and Nanomechanical Function of Self-Organizable Dendronized Polymethacrylates and Polyacrylates. *Macromolecules* **2017**, *50*, 5271−5284.

(11) (a) Percec, V.; Dulcey, A. E.; Balagurusamy, V. S. K.; Miura, Y.; Smidrkal, J.; Peterca, M.; Nummelin, S.; Edlund, U.; Hudson, S. D.; Heiney, P. A.; Duan, H.; Magonov, S. N.; Vinogradov, S. A. Self-Assembly of Amphiphilic Dendritic Dipeptides into Helical Pores. *Nature* **2004**, *430*, 764−768. (b) Percec, V.; Dulcey, A. E.; Peterca, M.; Ilies, M.; Sienkowska, M. J.; Heiney, P. A. Programming the Internal Structure and Stability of Helical Pores Self-Assembled from Dendritic Dipeptides *via* the Protective Groups of the Peptide. *J. Am. Chem. Soc.* **2005**, *127*, 17902−17909. (c) Percec, V.; Dulcey, A. E.; Peterca, M.; Ilies, M.; Ladislaw, J.; Rosen, B. M.; Edlund, U.; Heiney, P. A. The Internal Structure of Helical Pores Self-Assembled from Dendritic Dipeptides is Stereochemically Programmed and Allosterically Regulated. *Angew. Chem., Int. Ed.* **2005**, *44*, 6516−6521.

(12) Lugger, J. A. M.; Mulder, D. J.; Bhattacharjee, S.; Sijbesma, R. P. Homeotropic Self-Alignment of Discotic Liquid Crystals for Nanoporous Polymer Films. *ACS Nano* **2018**, *12*, 6714−6724.

(13) (a) Caspar, D. L. D. Movement and Self-Control in Protein Assemblies. Quasi-Equivalence Revisited. *Biophys. J.* **1980**, *32*, 103−135. (b) Percec, V.; Ahn, C.-H.; Ungar, G.; Yeardley, D. J. P.; Möller, M.; Sheiko, S. S. Controlling Polymer Shape through the Self-Assembly of Dendritic Side-Groups. *Nature* **1998**, *391*, 161−164.

(14) (a) Yeardley, D. J. P.; Ungar, G.; Percec, V.; Holerca, M. N.; Johansson, G. Spherical Supramolecular Minidendrimers Self-Organized in an 'Inverse Micellar'-like Thermotropic Body-Centered Cubic Liquid Crystalline Phase. *J. Am. Chem. Soc.* **2000**, *122*, 1684−1689. (b) Duan, H.; Hudson, S. D.; Ungar, G.; Holerca, M. N.; Percec, V. Definitive Support by Transmission Electron Microscopy, Electron Diffraction, and Electron Density Maps for the Formation of a BCC Lattice from Poly[*N*-[3,4,5-Tris(*n*-dodecan-l-yloxy)Benzoyl]-Ethyleneimine). *Chem. - Eur. J.* **2001**, *7*, 4134−4141.

(15) (a) Hudson, S. D.; Jung, H.-T.; Percec, V.; Cho, W.-D.; Johansson, G.; Ungar, G.; Balagurusamy, V. S. K. Direct Visualization of Individual Cylindrical and Spherical Supramolecular Dendrimers. *Science* **1997**, *278*, 449−452. (b) Percec, V.; Cho, W.; Möller, M.; Prokhorova, S. A.; Ungar, G.; Yeardley, D. J. P. Design and Structural Analysis of the First Spherical Monodendron Self-Organizable in a Cubic Lattice. *J. Am. Chem. Soc.* **2000**, *122*, 4249−4250. (c) Dukeson, D. R.; Ungar, G.; Balagurusamy, V. S. K.; Percec, V.; Johansson, G. A.; Glodde, M. Application of Isomorphous Replacement in the Structure Determination of a Cubic Liquid Crystal Phase and Location of Counterions. *J. Am. Chem. Soc.* **2003**, *125*, 15974−15980.

(16) (a) Sinha, A. K. Topologically Close-Packed Structures of Transition Metal Alloys. *Prog. Mater. Sci.* **1972**, *15*, 81−185. (b) Ungar, G.; Zeng, X. Frank−Kasper, Quasicrystalline and Related Phases in Liquid Crystals. *Soft Matter* **2005**, *1*, 95−106.

(17) Mariani, P.; Luzzati, V.; Delacroix, H. Cubic Phases of Lipid-Containing Systems. Structure Analysis and Biological Implications. *J. Mol. Biol.* **1988**, *204*, 165−189.

(18) Ungar, G.; Liu, Y.; Zeng, X.; Percec, V.; Cho, W.-D. Giant Supramolecular Liquid Crystal Lattice. *Science* **2003**, *299*, 1208−1211.

(19) (a) Zeng, X.; Ungar, G.; Liu, Y.; Percec, V.; Dulcey, A. E.; Hobbs, J. K. Supramolecular Dendritic Liquid Quasicrystals. *Nature* **2004**, *428*, 157−160. (b) Dotera, T. Quasicrystals in Soft Matter. *Isr. J. Chem.* **2011**, *51*, 1197−1205. (c) Zhang, R.; Zeng, X.; Ungar, G. Direct AFM Observation of Individual Micelles, Tile Decorations and Tiling Rules of a Dodecagonal Liquid Quasicrystal. *J. Phys.: Condens. Matter* **2017**, *29*, 414001.

(20) Malthete, J.; Jacques, J.; Huu Tinh, N.; Destrade, C. Macroscopic Evidence of Molecular Chirality in Columnar Mesophases. *Nature* **1982**, *298*, 46−48.

(21) Percec, V.; Aqad, E.; Peterca, M.; Rudick, J. G.; Lemon, L.; Ronda, J. C.; De, B. B.; Heiney, P. A.; Meijer, E. W. Steric Communication of Chiral Information Observed in Dendronized Polyacetylenes. *J. Am. Chem. Soc.* **2006**, *128*, 16365−16372.

(22) Alexander, J. Loxodromes: A Rhumb Way to Go. *Math. Mag.* **2004**, *77*, 349−356.

(23) Percec, V.; Peterca, M.; Dulcey, A. E.; Imam, M. R.; Hudson, S. D.; Nummelin, S.; Adelman, P.; Heiney, P. A. Hollow Spherical Supramolecular Dendrimers. *J. Am. Chem. Soc.* **2008**, *130*, 13079−13094.

(24) Glaser, R. Helical Stereochemistry. In *Symmetry, Spectroscopy, and Crystallography*; Wiley-VCH Verlag GmbH & Co. KGaA, 2015; pp 269−300.

(25) Ferrand, Y.; Huc, I. Designing Helical Molecular Capsules Based on Folded Aromatic Amide Oligomers. *Acc. Chem. Res.* **2018**, *51*, 970−977.

(26) Tourigny, D. S. The Theory of an Electron on a Loxodrome. *Mod. Phys. Lett. B* **2012**, *26*, 1250052.

(27) (a) Sahoo, D.; Peterca, M.; Aqad, E.; Partridge, B. E.; Heiney, P. A.; Graf, R.; Spiess, H. W.; Zeng, X.; Percec, V. Hierarchical Self-Organization of Perylene Bisimides into Supramolecular Spheres and Periodic Arrays Thereof. *J. Am. Chem. Soc.* **2016**, *138*, 14798−14807. (b) Sahoo, D.; Peterca, M.; Aqad, E.; Partridge, B. E.; Heiney, P. A.; Graf, R.; Spiess, H. W.; Zeng, X.; Percec, V. Tetrahedral Arrangements of Perylene Bisimide Columns *via* Supramolecular Orientational Memory. *ACS Nano* **2017**, *11*, 983−991.

(28) (a) Zeng, X.; Liu, F.; Fowler, A. G.; Ungar, G.; Cseh, L.; Mehl, G. H.; Macdonald, J. E. 3D Ordered Gold Strings by Coating Nanoparticles with Mesogens. *Adv. Mater.* **2009**, *21*, 1746−1750. (b) Cseh, L.; Mang, X.; Zeng, X.; Liu, F.; Mehl, G. H.; Ungar, G.; Siligardi, G. Helically Twisted Chiral Arrays of Gold Nanoparticles Coated with a Cholesterol Mesogen. *J. Am. Chem. Soc.* **2015**, *137*, 12736−12739.

(29) Guerra, S.; Iehl, J.; Holler, M.; Peterca, M.; Wilson, D. A.; Partridge, B. E.; Zhang, S.; Deschenaux, R.; Nierengarten, J.-F.; Percec, V. Self-Organisation of Dodeca-Dendronized Fullerene into

DOI: 10.1021/jacs.8b09174
J. Am. Chem. Soc. 2018, 140, 13478−13487

Supramolecular Discs and Helical Columns Containing a Nanowire-like Core. *Chem. Sci.* **2015**, *6*, 3393−3401.
(30) Sakya, P.; Seddon, J. M.; Templer, R. H.; Mirkin, R. J.; Tiddy, G. J. T. Micellar Cubic Phases and Their Structural Relationships: The Nonionic Surfactant System C12EO12/Water. *Langmuir* **1997**, *13*, 3706−3714.
(31) (a) Zimmermann, H.; Poupko, R.; Luz, Z.; Billard, J. Pyramidic Mesophases. *Zeitschrift für Naturforsch.* **2013**, *40a*, 149−160. (b) Malthete, J.; Collet, A. Liquid Crystals with a Cone-Shaped Cyclotriveratrylene Core. *Nouv. J. Chemie* **1985**, *9*, 151−153. (c) Levelut, A. M.; Malthete, J.; Collet, A. X-Ray Structural Study of the Mesophases of Some Cone-Shaped Molecules. *J. Phys. (Paris)* **1986**, *47*, 351−357. (d) Collet, A. Cyclotriveratrylenes and Cryptophanes. *Tetrahedron* **1987**, *43*, 5725−5759.
(32) (a) Peterca, M.; Percec, V.; Imam, M. R.; Leowanawat, P.; Morimitsu, K.; Heiney, P. A. Molecular Structure of Helical Supramolecular Dendrimers. *J. Am. Chem. Soc.* **2008**, *130*, 14840−14852. (b) Peterca, M.; Imam, M. R.; Hudson, S. D.; Partridge, B. E.; Sahoo, D.; Heiney, P. A.; Klein, M. L.; Percec, V. Complex Arrangement of Orthogonal Nanoscale Columns *via* a Supramolecular Orientational Memory Effect. *ACS Nano* **2016**, *10*, 10480−10488.
(33) (a) Malthete, J.; Collet, A. Inversion of the Cyclotribenzylene Cone in a Columnar Mesophase: A Potential Way to Ferroelectric Materials. *J. Am. Chem. Soc.* **1987**, *109*, 7544−7545. (b) Poupko, R.; Luz, Z.; Spielberg, N.; Zimmermann, H. Structure and Dynamics of Pyramidic Liquid Crystals by Deuterium NMR and X-Ray Diffraction. *J. Am. Chem. Soc.* **1989**, *111*, 6094−6105. (c) Lesot, P.; Merlet, D.; Sarfati, M.; Courtieu, J.; Zimmermann, H.; Luz, Z. Enantiomeric and Enantiotopic Analysis of Cone-Shaped Compounds with C_3 and C_{3v} Symmetry Using NMR Spectroscopy in Chiral Anisotropic Solvents. *J. Am. Chem. Soc.* **2002**, *124*, 10071−10082. (d) Zimmermann, H.; Bader, V.; Poupko, R.; Wachtel, E. J.; Luz, Z. Mesomorphism, Isomerization, and Dynamics in a New Series of Pyramidic Liquid Crystals. *J. Am. Chem. Soc.* **2002**, *124*, 15286−15301. (e) Zimmermann, H.; Tolstoy, P.; Limbach, H. H.; Poupko, R.; Luz, Z. The Saddle Form of Cyclotriveratrylene. *J. Phys. Chem. B* **2004**, *108*, 18772−18778.
(34) (a) Kranig, W.; Spiess, H. W.; Zimmermann, H. Substituted Tetrabenzocyclophanes as Mesogenic Units of New Polycondensates Exhibiting Columnar Mesophases. *Liq. Cryst.* **1990**, *7*, 123−129. (b) Percec, V.; Cho, C. G.; Pugh, C. Alkyloxy-Substituted CTTV Derivatives That Exhibit Columnar Mesophases. *J. Mater. Chem.* **1991**, *1*, 217−222. (c) Kuebler, S. C.; Boeffel, C.; Spiess, H. W. Dynamics and Structure of a Flexible Columnar Liquid-Crystal Based on Tetrabenzocyclododecatetraene. *Liq. Cryst.* **1995**, *18*, 309−318.
(35) (a) Percec, V.; Cho, C. G.; Pugh, C. Cyclotrimerization versus Cyclotetramerization in the Electrophilic Oligomerization of 3,4-Bis(Methyloxy)Benzyl Derivatives. *Macromolecules* **1991**, *24*, 3227−3234. (b) Yamato, T.; Hideshima, C.; Prakash, G. K. S.; Olah, G. A. Solid Superacid-Catalyzed Organic Synthesis. 4. Perfluorinated Resinsulfonic Acid (Nafion-H) Catalyzed Friedel−Crafts Benzylation of Benzene and Substituted Benzenes. *J. Org. Chem.* **1991**, *56*, 2089−2091.
(36) Li, Y.; Lin, S.-T.; Goddard, W. A. Efficiency of Various Lattices from Hard Ball to Soft Ball: Theoretical Study of Thermodynamic Properties of Dendrimer Liquid Crystal from Atomistic Simulation. *J. Am. Chem. Soc.* **2004**, *126*, 1872−1885.
(37) Yao, X.; Cseh, L.; Zeng, X.; Xue, M.; Liu, Y.; Ungar, G. Body-Centred Cubic Packing of Spheres − The Ultimate Thermotropic Assembly Mode for Highly Divergent Dendrons. *Nanoscale Horiz* **2017**, *2*, 43−49.
(38) Orwoll, R. A.; Flory, P. J. Equation-of-State Parameters for Normal Alkanes. Correlation with Chain Length. *J. Am. Chem. Soc.* **1967**, *89*, 6814−6822.
(39) Shcherbina, M. A.; Zeng, X.; Tadjiev, T.; Ungar, G.; Eichhorn, S. H.; Phillips, K. E. S.; Katz, T. J. Hollow Six-Stranded Helical Columns of a Helicene. *Angew. Chem., Int. Ed.* **2009**, *48*, 7837−7840.
(40) Rosen, B. M.; Peterca, M.; Huang, C.; Zeng, X.; Ungar, G.; Percec, V. Deconstruction as a Strategy for the Design of Libraries of Self-Assembling Dendrons. *Angew. Chem., Int. Ed.* **2010**, *49*, 7002−7005.
(41) Percec, V.; Holerca, M. N.; Uchida, S.; Cho, W. D.; Ungar, G.; Lee, Y.; Yeardley, D. J. P. Exploring and Expanding the Three-Dimensional Structural Diversity of Supramolecular Dendrimers with the Aid of Libraries of Alkali Metals of Their AB_3 Minidendritic Carboxylates. *Chem. - Eur. J.* **2002**, *8*, 1106−1117.
(42) (a) Rowan, A. E.; Nolte, R. J. M. Helical Molecular Programming. *Angew. Chem., Int. Ed.* **1998**, *37*, 63−68. (b) Yashima, E.; Ousaka, N.; Taura, D.; Shimomura, K.; Ikai, T.; Maeda, K. Supramolecular Helical Systems: Helical Assemblies of Small Molecules, Foldamers, and Polymers with Chiral Amplification and Their Functions. *Chem. Rev.* **2016**, *116*, 13752−13990.
(43) Percec, V.; Leowanawat, P. Why Are Biological Systems Homochiral? *Isr. J. Chem.* **2011**, *51*, 1107−1117.
(44) Roche, C.; Sun, H.-J.; Leowanawat, P.; Araoka, F.; Partridge, B. E.; Peterca, M.; Wilson, D. A.; Prendergast, M. E.; Heiney, P. A.; Graf, R.; Spiess, H. W.; Zeng, X.; Ungar, G.; Percec, V. A Supramolecular Helix That Disregards Chirality. *Nat. Chem.* **2016**, *8*, 80−89.
(45) (a) Rosen, B. M.; Wilson, D. A.; Wilson, C. J.; Peterca, M.; Won, B. C.; Huang, C.; Lipski, L. R.; Zeng, X.; Ungar, G.; Heiney, P. A.; Percec, V. Predicting the Structure of Supramolecular Dendrimers *via* the Analysis of Libraries of AB_3 and Constitutional Isomeric AB_2 Biphenylpropyl Ether Self-Assembling Dendrons. *J. Am. Chem. Soc.* **2009**, *131*, 17500−17521. (b) Tomalia, D. A.; Khanna, S. N. A Systematic Framework and Nanoperiodic Concept for Unifying Nanoscience: Hard/Soft Nanoelements, Superatoms, Meta-Atoms, New Emerging Properties, Periodic Property Patterns, and Predictive Mendeleev-like Nanoperiodic Tables. *Chem. Rev.* **2016**, *116*, 2705−2774.
(46) Percec, V.; Dulcey, A. E.; Peterca, M.; Ilies, M.; Nummelin, S.; Sienkowska, M. J.; Heiney, P. A. Principles of Self-Assembly of Helical Pores from Dendritic Dipeptides. *Proc. Natl. Acad. Sci. U. S. A.* **2006**, *8*, 2518−2523.

DOI: 10.1021/jacs.8b09174
J. Am. Chem. Soc. 2018, 140, 13478−13487